Automatic Identification of *Mycobacterium tuberculosis* in Ziehl-Neelsen Stained Sputum Smear Microscopy Images using a Two-stage Classifier

Lucas de Assis Soares, Klaus Fabian Coco, Evandro Ottoni Teatini Salles and Saulo Bortolon
Federal University of Espirito Santo, 514 Fernando Ferrari Av., Vitoria, Brazil

Keywords: Automatic Microscopy, Tuberculosis, Ziehl-Neelsen, Bacilloscopy.

Abstract: This paper presents a method for the automatic identification of *Mycobacterium tuberculosis* in Ziehl-Neelsen stained sputum smear microscopy images, the most common bacilloscopy method in developing countries due to its low costs. The proposed method is divided in two stages: a projection of the original coloured image followed by the segmentation and the elimination of large and small segmented structures, and the classification of structures using neural networks and support vector machines. The segmentation of structures presents a loss of bacilli of 1.31 %, while the elimination of areas increases the loss to 14.39 %. The evaluation of the classification of structures is made using cross validation and a maximum sensitivity of 94.25 % is obtained. The presented method has a low computational cost, allying performance and efficiency.

1 INTRODUCTION

Tuberculosis (TB) is a major global health problem. According to the Global Tuberculosis Report 2014 (WHO, 2014), in 2013 an estimated 9 million people developed TB and 1.5 million died from the disease. The disease is second only to HIV/AIDS as the greatest killer worldwide due to a single infectious agent. The number of TB deaths is unacceptably large since the disease is preventable and treatable. Due to the large occurrence, the disease remains a major global health problem (WHO, 2014).

The most common method for diagnosis of tuberculosis in developing countries is sputum smear microscropy, in which a sample of sputum is collected, stained and examined under a microscope by a trained laboratory technician (WHO, 2014).

Two techniques are used for tuberculosis diagnosis using sputum smear microscopy: fluorescence microscopy and conventional microscopy.

Fluorescence microscopy has a greater sensitivity rate than conventional microscopy but also has greater costs associated with it, so that it is not often available in developing countries where conventional microscopy using the Ziehl-Neelsen method is the most common technique used for the diagnosis of tuberculosis in those countries (Costa Filho et al., 2012), (Desikan, 2013).

For the tuberculosis diagnosis, the laboratory technician must meticulously examine each slide looking for bacilli and then record the number of bacteria observed in the slide. This process is labor intensive and time consuming (Smart, 2007). For this reason, it is interesting to have an automatic system capable of analyzing a picture taken by a microscope and identify tuberculosis bacteria on it.

In the field of conventional microscopy, Sadaphal et al., 2008, proposed the segmentation based on Bayesian analysis and the classification of structures using a decision tree considering major axis length and eccentricity. Costa et al., 2008, proposed the segmentation in the image given by the operation $R-G$, using an adaptive threshold to global segmentation. In Sotaquir et al., 2009, it is proposed a segmentation based on the colour spaces YcbCr and Lab. Makkapati et al., 2009, presented a method for bacilli recognition segmenting the image using Otsu's technique and searching for a beaded structure inside the segmented objects in order to classify them. Nayak et al., 2010, proposed the segmentation based on minimum distance between clusters of bacilli pixels and non-bacilli pixels in the colour space HSV. Zhai et al., 2010, proposed the segmentation based on the colour spaces HSI and Lab followed by a decision tree to classify the segmented objects using area, roughness and circularity.

In more recent works, Siena et al., 2012, proposed k-means clustering segmentation followed by the classification of the structures using a multilayer perceptron neural network considering eccentricity

Soares L., Coco K., Salles E. and Bortolon S..
Automatic Identification of Mycobacterium tuberculosis in Ziehl-Neelsen Stained Sputum Smear Microscopy Images using a Two-stage Classifier.
DOI: 10.5220/0005345201860191
In *Proceedings of the 10th International Conference on Computer Vision Theory and Applications* (VISAPP-2015), pages 186-191
ISBN: 978-989-758-091-8

and compacity. Costa Filho et al., 2012, segmented the images using information from the colour spaces RGB, HSI, YcbCr and Lab in a multilayer perceptron neural network. For the classification of the structures, eccentricity and color ratio were used in a decision tree. Kusworo et al., 2013, presented a method using Otsu segmentation technique on the hue component of the HSV colour space and using eccentricity, compacity and metric in a multilayer perceptron neural network. Chayadevi and Raju, 2014, proposed the segmentation of images using watershed in the colour spaces YcbCr, HSI and Lab.

This paper proposes a method for automatic bacilli recognition in Ziehl-Neelsen stained sputum images based on an improved technique for segmentation of the images and the use of diverse characteristics for the classification of the structures.

The rest of this paper is organized as follows: In Section 2 the materials and methods used are presented, in Section 3 the results are presented and discussed, and in Section 4 the conclusion is presented.

2 MATERIAL AND METHODS

The image set used in this work was the one used in Costa Filho et al., 2012,. The data set consists of 120 images a size of 2816 x 2112 pixels of sputum smear microscopy slides from 12 patients prepared using Kinyoun acid-fast stain and counterstained with methylene blue solution. The images were taken using a numerical aperture of 1.25 and a magnification of 100x combined with an optical zoom of 4x. The images can be accessed in *http://www.tbimages.ufam.edu.br* (CETELI, 2014).

The proposed method consists of two stages. First, the coloured image is projected into a gray scale image. The projection is based on Fisher linear discriminant. After the projection, the image is segmented and the threshold is calculated according to the mean intensity of the gray scale image. The second stage consists of an area analysis of the segmented structures and the classification of the remaining structures using a feedforward neural network and a support vector machine. The parameters used for classification were eccentricity, circularity, invariant moments, Fourier descriptors, and the mean and the standard deviation of each colour channel of the pixels in the structure. Figure 1 presents the block diagram of the proposed method.

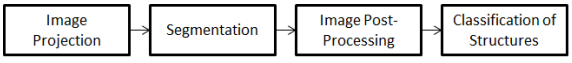

Figure 1: Block diagram showing the proposed method.

Fisher linear discriminant seeks to find the projection vector that maximizes the criterion given by

$$J(w) = \frac{w^t S_B w}{w^t S_W w}, \quad (1)$$

where S_B is the between-class scatter matrix and is a measure of the distance between the means of the two classes,S_W is the within-class scatter matrix and can be understood as the scatter of the samples around their respective class means, and w is the 3-dimensional projection vector. (Duda et al., 2001). Maximizing $J(w)$ is then equivalent to maximizing S_B while minimizing S_W.

In this case the background pixel vectors considered were the ones for which the hue component is smaller than 0.2 or greater than 0.7, since this is the hue range where the bacilli pixels belong. This selection was made so that the background pixel vectors were from a single probability distribution.

With the projection vector found, every pixel vector is projected and a gray intensity image is generated. After the projection, a global thresholding is applied for image segmentation. The threshold is defined based on the mean intensity of the projected image according to a first degree polynomial defined through linear regression.

In the segmented image there are some structures that are too small or too big to be a bacilli. Some of those structures may be a clustering of bacilli, but when there is a cluster of them, there are normally many bacilli present in the image, so individual bacilli are also present. Structure containing less than 200 pixels or more than 2,600 pixels were discarded. The removal of structures with area smaller than 200 pixels was made according to (Costa et al., 2008). For the upper limit, it was noted that more than 95 % of the structures had an area smaller than 2,600 pixels.

The next step is to classify those structures. The parameters used for classification were eccentricity, circularity, invariant moments (Gonzalez and Woods, 2007), Fourier descriptors and the mean and the standard deviation of each color channel of the pixels in the structure. The Fourier descriptors used were the ones proposed in Costa and Cesar Jr, 2000, so that all features used were invariant to translation, rotation, and scaling.

These features were applied to a multilayer perceptron neural network (Haykin et al., 2009) and a support vector machine (Bishop et al., 2006) to classify the structures in two groups: bacilli and non-bacilli. The neural network was trained using the Levenberg-Marquardt algorithm. The classifiers were evaluated using 10-fold cross validation (Witten and Frank, 2005).

3 RESULTS AND DISCUSSION

In the first stage of the proposed method, the image data set was divided into two groups consisting of sixty images each: a training set and a test set. Figure 2 shows some of the images used in the test set. The images vary in the number of bacilli and the number of other structures present in the images.

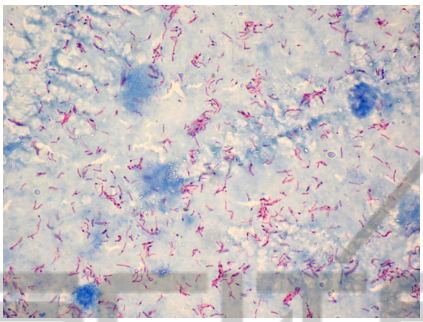

(a)

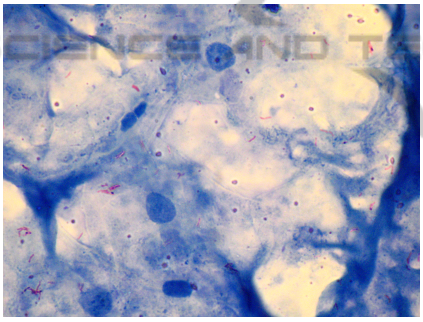

(b)

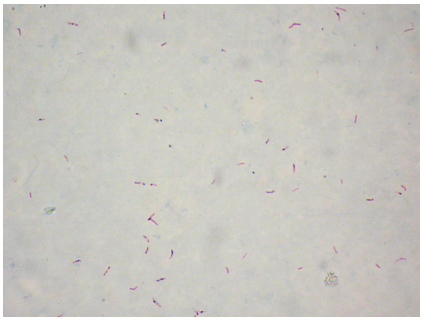

(c)

Figure 2: Examples from the image set.

The projection vector found through Fisher linear discriminant is

$$w = [0.5640, -0.8249, -0.0384], \quad (2)$$

which is equivalent to say that for every pixel in the original image, we have the linear transformation given by

$$I = 0.5640R - 0.8249G - 0.0384B, \quad (3)$$

where I is the new value of the pixel and R, G, and B are the red, green, and blue components of the pixel, respectively.

The projection of the original images shown in Figure 2 are presented in correspondence in Figure 3. It can be seen that bacilli appear as bright structures in comparison with the other structures in the image. Figure 4 presents the histogram of the two classes of each image, showing the increased separability between the classes.

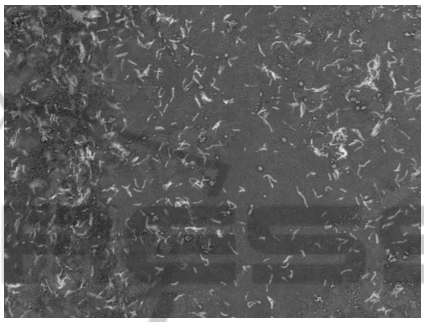

(a)

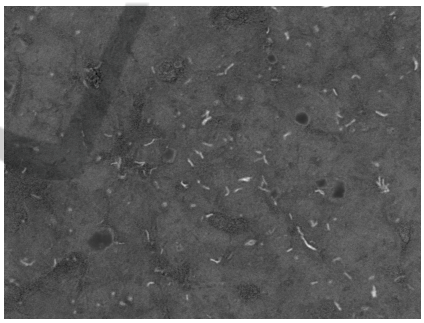

(b)

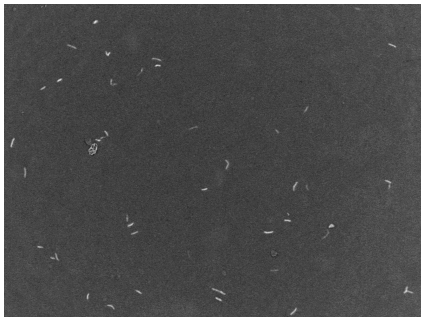

(c)

Figure 3: Projection of the images shown in Figure 2.

A linear projection has a low computational cost and, as can be seen in Figures 3 and 4, provides a good separability between bacilli and background, which benefits the process of segmentation.

In order to define the threshold for the global thresholding segmentation, the mean intensity of the gray scale image was used. The threshold that sepa-

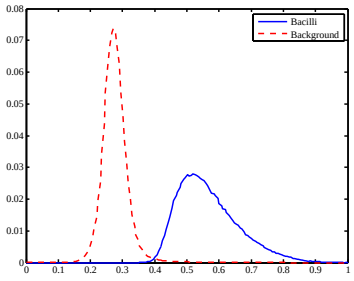

(a)

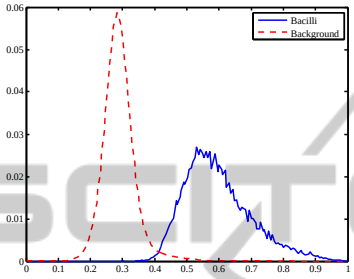

(b)

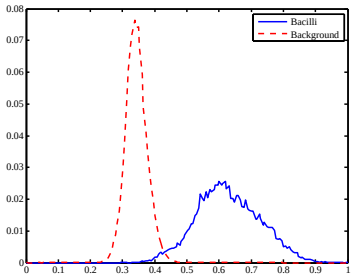

(c)

Figure 4: Histogram of the imagens shown in Figure 3. The blue continuous line indicates bacilli, while the red dashed line indicates non-bacilli (background) pixels.

rates a bacilli pixel from a non-bacilli pixels was defined as the point where the histograms of the two classes touch each other. It is observed that the relation between the threshold and the mean intensity is approximately linear as shown in Figure 5. Therefore a linear regression was performed using the data from the training set and the first order polynomial obtained is given by

$$threshold = 0.8363\mu + 0.1444, \quad (4)$$

where the mean intensity is represented by μ.

Again, the calculus of the mean intensity of a gray intensity image and its application in a first order polynomial have a low computational cost.

With the projection vector and the first order polynomial it is possible to segment the image. Figure 6

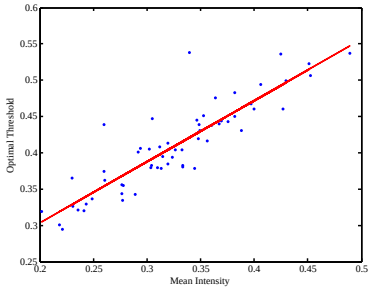

Figure 5: Linear relation between the mean intensity of the projected image and the optimal threshold. The continuous line shows the polynomial obtained through linear regression.

shows the segmented images of the images shown in Figure 2. For the test set, 98.69% of the bacilli present in the images were segmented, in comparison with a loss of 1.31%. Since another classification stage follows the segmentation stage, the only measure to evaluate the segmentation was the number of bacilli segmented in comparison with the percentage of bacilli lost.

The structures are then filtered according to their area. Structures with an area smaller than 200 pixels or greater than 2,600 pixels are not considered in the rest of the classification process. After this morphological analysis, 85.61% of the bacilli present in the test set were segmented in comparison with a loss of 14.39% of bacilli not segmented.

The increase of bacilli lost is mainly due to the elimination of structures with a large area, because the bacilli appear as large bacilli clusters in the images. However, in the image set, the large clusters of bacilli appears in the images containing a great number of bacilli, where individual bacilli also appear. For this reason, the identification of bacilli in the images is still guaranteed by the system. The small structures appear when bacilli are partially identified in the image, mainly due to the focus adjustment made before the images were taken. Despite the increase on the loss of bacilli, the elimination of structures with small and large areas is still important to reduce the variability of the structures for the next stage.

For the classification of the structures, a k-fold cross validation method was employed in order to evaluate the data using different training and test sets. A multilayer perceptron neural network with one hidden layer with twenty neurons and a support vector machine with a polynomial kernel function of order 5 were used. In the neural network, the hidden layer uses a sigmoid transfer function as its activation function while the output layer uses a linear function. The sensitivity, specificity, accuracy and precision obtained using the neural network are summarized in Ta-

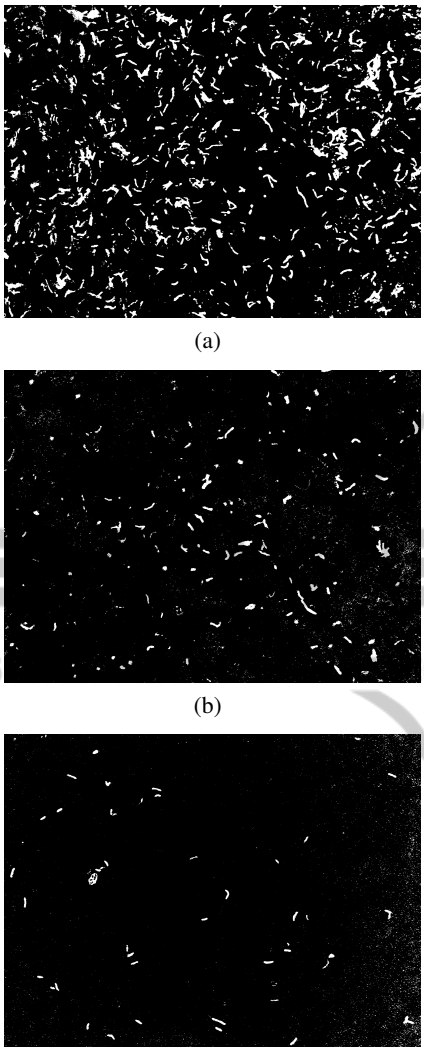

(a) (b) (c)

Figure 6: Segmentation of the images shown in Figure 3.

ble 1, showing the maximum, minimum and mean results obtained. The same results for the support vector machine are summarized in Table 2.

Table 1: Results from cross validation of the classification of segmented structures using neural networks.

	Mean	Maximum	Minimum
Sensitivity	86.84 %	94.25 %	79.94 %
Specificity	87.93 %	94.71 %	82.37 %
Accuracy	94.02 %	95.73 %	92.31 %
Precision	88.22 %	92.50 %	81.25 %

The results for sensitivity were greater using neural networks, even though the results using the two different classifiers were quite similar. The similarity between the results indicate that the used features provide a good representation of the structures of each class allowing for an efficient distinction between the classes.

Table 2: Results from cross validation of the classification of segmented structures using support vector machines.

	Mean	Maximum	Minimum
Sensitivity	86.24 %	93.35 %	79.23 %
Specificity	88.24 %	95.33 %	82.36 %
Accuracy	94.16 %	95.70 %	92.42 %
Precision	86.79 %	91.84 %	79.65 %

It is not possible to compare the segmentation results of this paper with the work done in (Costa Filho et al., 2012) since the ground truth used for segmentation is different. In the former, the evaluation is done considering the number of bacilli segmented ignoring the segmented pixels that do not belong to bacilli, while in the last the pixels are evaluated individually. However, the proposed method involves a linear projection followed by a first order polynomial evaluation and a global thresholding, which is faster than the neural network used in (Costa Filho et al., 2012), and it is not subject to overtraining problems that neural networks may suffer from.

Even though the segmentation part can not be compared with (Costa Filho et al., 2012), it is possible to compare the classification of the segmented structures. In (Costa Filho et al., 2012) the classification of structures is evaluated considering sensitivity, precision and false detection, where false detection is defined as the ratio of the quantity of noise classified as bacilli and number of objects classified as bacilli, being equivalent to $(1 - precision)$. Table 3 compares the results between obtained in (Costa Filho et al., 2012) and the ones achieved in this paper, where the best results of both papers were considered. It should be noted however that cross validation was not used in the former.

The images used in other works were not accessible so it was not possible to implement the methodology presented in this paper using those images and compare the results.

4 CONCLUSION

Even though the automatic identification of bacilli in sputum smear Ziehl-Neelsen stained images is a difficult task, the proposed method shows that it can be achieved efficiently and with a low computational cost.

The main contributions from this paper were the proposal of a linear projection method based on Fisher discriminant analysis and the segmentation based on a first order polynomial that allows the im-

Table 3: Results comparison between this paper and the one published in (Costa Filho et al., 2012).

Publication	Sensitivity (%)	Precision (%)	False detection (%)
Present paper	94.25	92.50	7.50
Costa Filho et al., 2012	91.53	91.49	8.51

ages segmentation to be fast, and the application of cross validation to analyze the effectiveness of the classification of the structures.

ACKNOWLEDGEMENTS

The authors would like to acknowledge the financial support received from the National Council for Scientific and Technological Development CNPq, Brazil. The authors also gratefully acknowledge CAPES (Brazil) by the financial support to attend at VISAPP 2015.

REFERENCES

Bishop, C. M. et al. (2006). *Pattern recognition and machine learning*, volume 1. springer New York.

CETELI (2014). An image database of conventional sputum smear microscopy for tuberculosis. Center for Research and Development in Electronic and Information Technology. http://http://www.tbimages.ufam.edu.br/.

Chayadevi, M. and Raju, G. (2014). Automated colour segmentation of tuberculosis bacteria thru region growing: A novel approach. In *Applications of Digital Information and Web Technologies (ICADIWT), 2014 Fifth International Conference on the*, pages 154–159. IEEE.

Costa, L. F. and Cesar Jr, R. M. (2000). *Shape analysis and classification: theory and practice*. CRC press.

Costa, M. G., Costa Filho, C. F., Sena, J. F., Salem, J., and de Lima, M. O. (2008). Automatic identification of mycobacterium tuberculosis with conventional light microscopy. In *Engineering in Medicine and Biology Society, 2008. EMBS 2008. 30th Annual International Conference of the IEEE*, pages 382–385. IEEE.

Costa Filho, C. F. F., Levy, P. C., Xavier, C. M., Costa, M. G., Fujimoto, L. B., and Salem, J. (2012). Mycobacterium tuberculosis recognition with conventional microscopy. In *Engineering in Medicine and Biology Society (EMBC), 2012 Annual International Conference of the IEEE*, pages 6263–6268. IEEE.

Desikan, P. (2013). Sputum smear microscopy in tuberculosis: Is it still relevant? volume 137, pages 442–444.

Duda, R. O., Hart, P. E., and Stork, D. G. (2001). *Pattern classification*. Wiley, 2nd edition.

Gonzalez, R. C. and Woods, R. E. (2007). *Digital Image Processing*. Prentice Hall, 3rd edition.

Haykin, S. S., Haykin, S. S., Haykin, S. S., and Haykin, S. S. (2009). *Neural networks and learning machines*, volume 3. Pearson Education Upper Saddle River.

Kusworo, A., Rahmat, G., Aris, S., Adi, P., Ari, B., and Nelly, M. (2013). Autothresholding segmentation for tuberculosis bacteria identification in the ziehl-neelsen sputum sample. In *Proceedings The 7th International Conference on Information & Communication Technology and Systems (ICTS)*, pages 15–16.

Makkapati, V., Agrawal, R., and Acharya, R. (2009). Segmentation and classification of tuberculosis bacilli from zn-stained sputum smear images. In *Automation Science and Engineering, 2009. CASE 2009. IEEE International Conference on*, pages 217–220. IEEE.

Nayak, R., Shenoy, V. P., and Galigekere, R. R. (2010). A new algorithm for automatic assessment of the degree of tb-infection using images of zn-stained sputum smear. In *Systems in Medicine and Biology (ICSMB), 2010 International Conference on*, pages 294–299. IEEE.

Sadaphal, P., Rao, J., Comstock, G., and Beg, M. (2008). Image processing techniques for identifying mycobacterium tuberculosis in ziehl-neelsen stains [short communication]. *The International Journal of Tuberculosis and Lung Disease*, 12(5):579–582.

Siena, I., Adi, K., Gernowo, R., and Miransari, N. (2012). Development of algorithm tuberculosis bacteria identification using color segmentation and neural networks. *International Journal of Video and Image Processing and Network Security*, 12(4):9–13.

Smart, T. (2007). Background on smear microscopy in tb diagnosis. http://www.aidsmap.com/Background-on-smear-microscopy-in-TB-diagnosis/page/1426650/.

Sotaquirá, M., Rueda, L., and Narvaez, R. (2009). Detection and quantification of bacilli and clusters present in sputum smear samples: a novel algorithm for pulmonary tuberculosis diagnosis. In *Digital Image Processing, 2009 International Conference on*, pages 117–121. IEEE.

WHO (2014). Tuberculosis (tb). World Health Organization. http://www.who.int/tb/.

Witten, I. H. and Frank, E. (2005). *Data Mining: Practical machine learning tools and techniques*. Morgan Kaufmann.

Zhai, Y., Liu, Y., Zhou, D., and Liu, S. (2010). Automatic identification of mycobacterium tuberculosis from zn-stained sputum smear: Algorithm and system design. In *Robotics and Biomimetics (ROBIO), 2010 IEEE International Conference on*, pages 41–46. IEEE.